Electronic Supplementary Material (ESI) for Sustainable Energy & Fuels.

Electronic Supplementary Information (ESI)

High performance binder-free Fe-Ni hydroxides on nickel foam prepared in piranha solution for oxygen evolution reaction

Cheol-Hwan Shin,[a] *Yi Wei,*[a] *Gisang Park,*[a] *Joonhee Kang*[b] *and Jong-Sung Yu*[a]*

[a] Department of Energy Science and Engineering, Daegu Gyeongbuk Institute of Science and Technology (DGIST), Daegu, 42988, Republic of Korea

[b] Platform Technology Laboratory, Korea Institute of Energy Research (KIER), Daejeon, 34129, Republic of Korea

Corresponding Author: jsyu@dgist.ac.kr

Materials. Nickel foam (NF) (thickness is 0.8 mm) was purchased from Wellcos corp. in Korea. Ruthenium (IV) dioxide (RuO_2 99.9%) was obtained from Alfa Aesar. 5 % Nafion, isopropanol (99.5%), hydrochloric acid (HCl, 37%), sulfuric acid (H_2SO_4, 95~98 %), hydrogen peroxide (H_2O_2, 30 wt% in H_2O) and iron (III) nitrate nonahydrate ($Fe(NO_3)_3{\cdot}9{\cdot}H_2O$, 99.5%) were purchased from Sigma-Aldrich in Korea. Ultra-purified de-ionized (DI) water was used for all experiment. A Piranha solution was prepared by mixing the H_2SO_4 and H_2O_2 with the volume ratio of $H_2SO_4 : H_2O_2 = 3:1$ (*Caution: Piranha solution is strong oxidation reagent).

Preparation of Fe-Ni electrocatalysts and RuO_2 electrode. First, NF was cut into 2 x 5 cm^2 and washed by 2.0 M HCl, ethanol and then water in sequence with sonication for 20 min, respectively. Washed NF was kept in vacuum oven at 60 °C during overnight. The clean NF was immersed in 80 ml of 12.5 mM $Fe(NO_3)_3{\cdot}9\ H_2O$ dissolved in 0.1 vol% piranha solution for different time duration of 0.5, 1 and 3 h, followed by washing with ethanol and water. The treated NF was dried in vacuum oven at 60 °C during overnight to get a NF-Fe-PS sample. A Fe-free NF sample, NF-PS, was also synthesized by using Fe-free piranha solution alone. In addition, several other samples were also prepared in different reaction media such as water, H_2O_2 or H_2SO_4, in which Fe^{3+} is included or not, with other experimental conditions kept identical to examine the effect of reaction medium and Fe species on the properties of resulting NF-based electrocatalysts and OER performance.

The RuO_2 electrode was prepared by drop casting method. RuO_2 nanoparticles were dispersed in a mixture solution of 0.84 g H_2O, 0.38 g isopropanol and 0.33g 5 % Nafion. After homogeneous mixing, 0.4 ml of RuO_2 slurry was dropped on both sides of NF (1x1 cm^2, pre-washed) and dried in vacuum oven at 60 °C during overnight. The loading amount of RuO_2 was around 0.2 mg/cm^2.

Preparation of $Fe(OH)_3$ powder. 0.1 g of $Fe(NO_3)_3{\cdot}9\ H_2O$ was dissolved in 50 ml of DI water and stirred for 10 min until the solution color was transparent. Next, 2 ml of 2.0 M NaOH aqueous solution was added to above-prepared solution with stirring for 30 min. Final product was collected by centrifugation and washed by DI water several times before drying in vacuum oven at 60 °C during overnight.

Material characterization. X-ray diffraction (XRD) was analyzed on a Rigaku Smartlab diffractometer with Cu Kα radiation (λ = 1.55406 Å) generated at 40 kV and 15mA and scanning rate of 4°/min. Scanning electron microscope (SEM) was obtained on a Hitachi-SU8230 at 3 kV. Transmission electron microscope (TEM) was measured on a Hitachi HF-3300 with acceleration voltage of 300 kV. The sample was prepared by vertically cutting the treated NF by forced ion beam (FIB) or scratching the NF surface. Energy dispersion spectroscopy (EDS) and elemental mapping were also performed on both SEM and TEM instruments. X-ray photoelectron spectroscopy (XPS) was performed using an ESCALAB 250 XPS system with a monochromated A1 Kα (150W) source. The obtained signals were corrected by C 1s at 284.8 eV as a calibration point. The energy scale was aligned by using the Fermi level of carbon in the XPS instrument (4.10 eV versus absolute vacuum value).

DFT calculation. All free energy calculations were performed using the Vienna ab-initio simulation package (VASP) based on a generalized gradient approximation with on-site Coulomb repulsion (Hubbard U correction).[1] The effective U-J terms were 3.5 and 6.6 eV for Fe and Ni, respectively.[2] The Perdew-Burke-Ernzerhof (PBE) exchange-correlation was used. The plane-wave cutoff energy was 500 eV and a Monkhorst-Pack 3x3x1 *k*-points scheme was applied to integrate the Brillouin zone. The atomic positions within the topmost hydroxide layer of the slabs were allowed to relax until the forces acting on all atoms were less than 0.02 eV $Å^{-1}$ with the energy convergence criterion of 10^{-5} eV. The DFT-D3 method of Grimme was employed to include the van der Waals interactions.[3] The adsorption free energies (ΔG) of the intermediates were obtained according to Equation (1)

Equation (1)

$$\Delta G = \Delta E + \Delta ZPE - T\Delta S + eU$$

where ΔE, ΔZPE, T, ΔS, and eU are the adsorption energy, the zero-point energy, temperature (298 K), entropy, and applied potential, respectively. The values of $\Delta ZPE - T\Delta S = 0.30$, 0.05 and 0.32 eV for OH*, O*, and OOH* formation were used for correction.

Electrochemical measurement for oxygen evolution reaction. Electrochemical performance for oxygen evolution reaction (OER) was carried out on a VSP potentiostat (Bio-Logic SAS) with a standard three-electrode cell in 1.0 M KOH (pH = 14). Hg/HgO filled with 1.0 M NaOH and Pt coil were used as the reference and counter electrodes, respectively, with applied varying bias. For powder samples, a catalyst ink was prepared by dispersing 5 mg of each catalyst powder into a mixture solution of 100 μl of 5% Nafion and 400 μl 50% ethanol solution. Glassy carbon electrode (GCE, diameter: 3 mm) coated with each catalyst ink was used as a working electrode, and Hg/HgO filled with 1.0 M NaOH and Pt wire were used as the reference and counter electrodes, respectively. The catalyst loading amount was controlled to 0.2 mg/cm^2.

The potential conversion from Hg/HgO to reversible hydrogen electrode (RHE) was performed according to Equation (1). Linear sweep voltammetry (LSV) and cycle voltammetry (CV) were performed with scan rates of 10 and 20 mV/s, respectively. 85 % iR compensation was applied to the obtained LSV curves according to Equation (2). Before measuring the electrochemical performance, CV was run for ∼ 20 times with a scan rate of 50 mV/s for stabilization. Tafel plots were calculated from corresponding LSV curves by Equation (3). The electrochemical impedance spectrum (ESI) was measured in a frequency range of 10^2-10^6 Hz with an AC voltage amplitude of 10 mV. Chronopotentiometric measurement was performed at 10 mA/cm^2 or 10~200 mA/cm^2 as step-applied current density. For calculation of double layer charge capacitance (C_{dl}), CV with various scan rates is conducted, and difference between anodic (j_a) and cathodic (j_c) currents at 0.65 V was determined to obtain C_{dl}. The slope of obtained curve is double layer charge capacitance (C_{dl}).

Equation (1)

$$E_{RHE} = E_{0(Hg/HgO,\ 1M\ NaOH)} + 0.059 \times pH + E_{applied}$$

where $E_{0(Hg/HgO,\ 1\ M\ NaOH)}$ = 0.118 V (vs. RHE). In this study, the pH value of 1.0 M KOH is considered as 14.

Equation (2)

$$E_{RHE.\ iR} = E_{RHE} - iR \times 0.85$$

where E_{RHE} is the applied potential vs RHE, i is the recorded current, and R is the solution resistance measured by EIS.

Equation (3)

$$\eta = b \cdot \log(j/j_0)$$

where η is the overpotential, b is the Tafel slope, j is the current density and j_0 is the exchange current density.

Solar cell power-driven water electrolysis. Two-electrode system comprising the as-prepared NF-based catalyst as a working electrode and Pt coil as both counter and reference electrode in 1.0 M KOH was constructed for solar cell power-driven water splitting. A commercial circular solar cell with 59 mm in diameter (5V, 40 mA) purchased from Solar Center Co. in Korea was connected to potentiostat and as-prepared working electrode by serial connection. 300 W Xe arc lamp (Newport Co.) with AM 1.5G filter was used as a light source and the intensity was controlled at 1 SUN. Chronoamperometric measurement was conducted for the sample powdered by the solar cell exposed to 1 SUN.

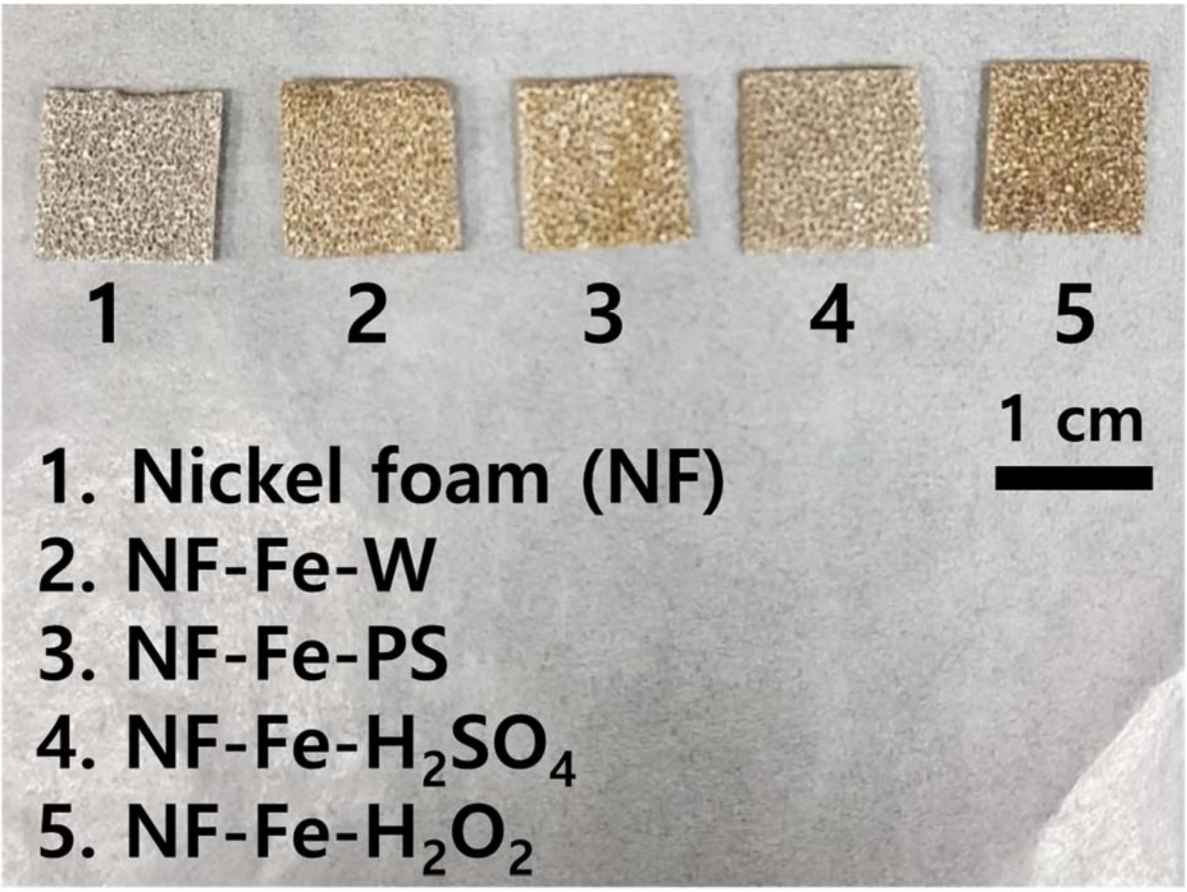

Fig. S1 Photographic images of as-prepared samples.

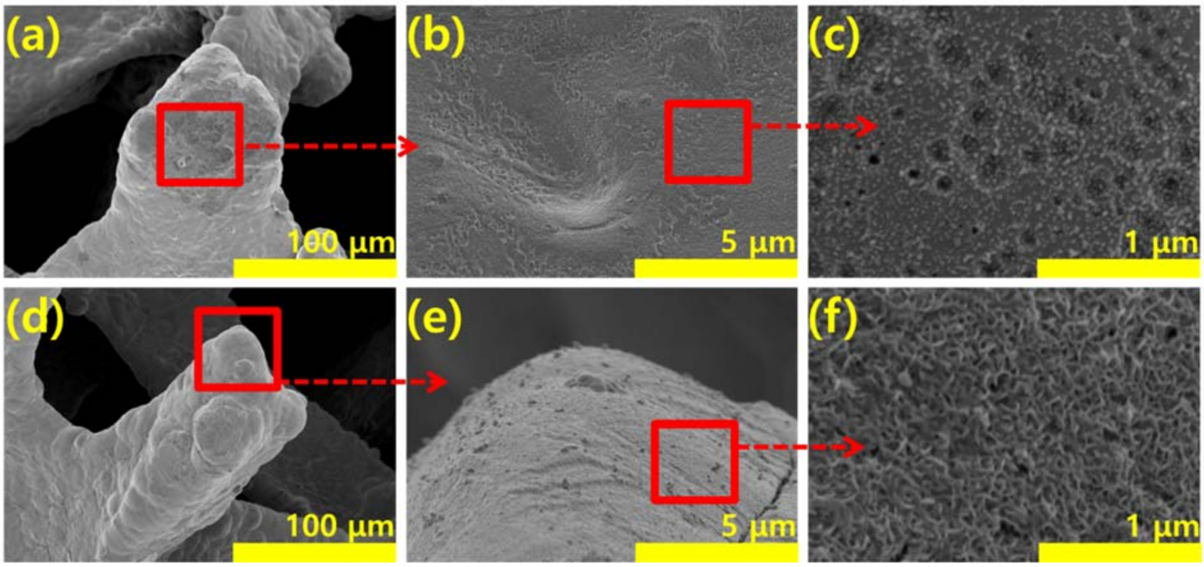

Fig. S2 SEM images of (a)-(c) NF-Fe-H_2O_2 and (d)-(f) NF-Fe-H_2SO_4 at different magnification.

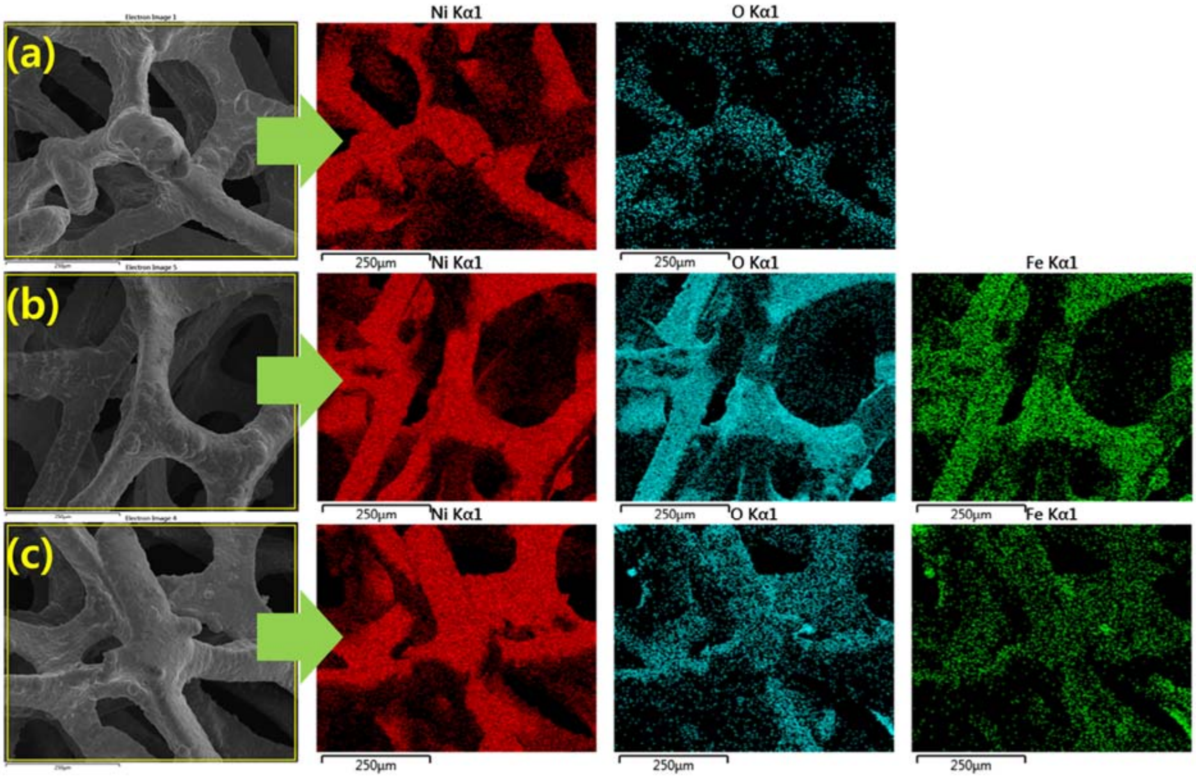

Fig. S3 Elemental mapping images of (a) NF, (b) NF-Fe-W and (c) NF-Fe-PS.

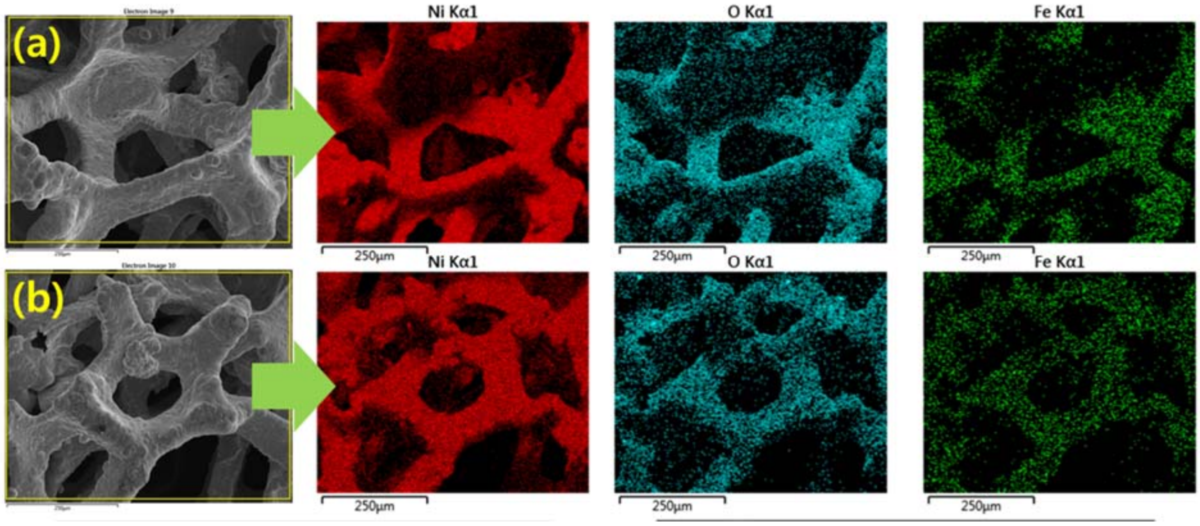

Fig. S4 Elemental mapping images of (a) NF-Fe-H_2O_2 and (b) NF-Fe-H_2SO_4.

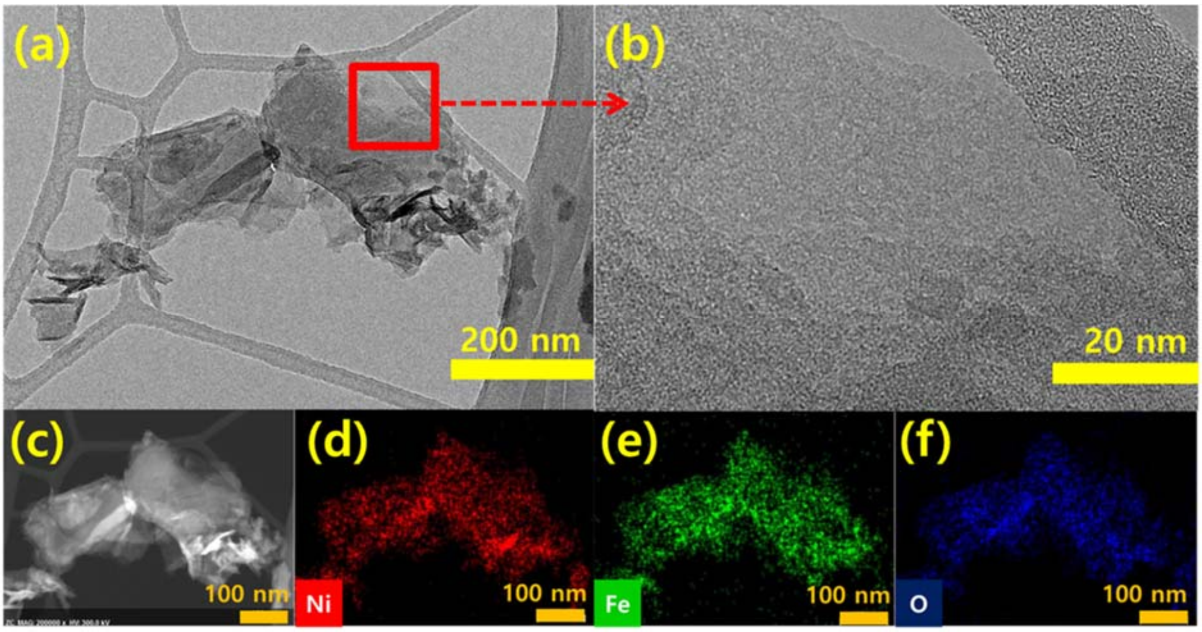

Fig. S5 TEM images of a broken piece of NF-Fe-PS along with corrospending elemental mapping images.

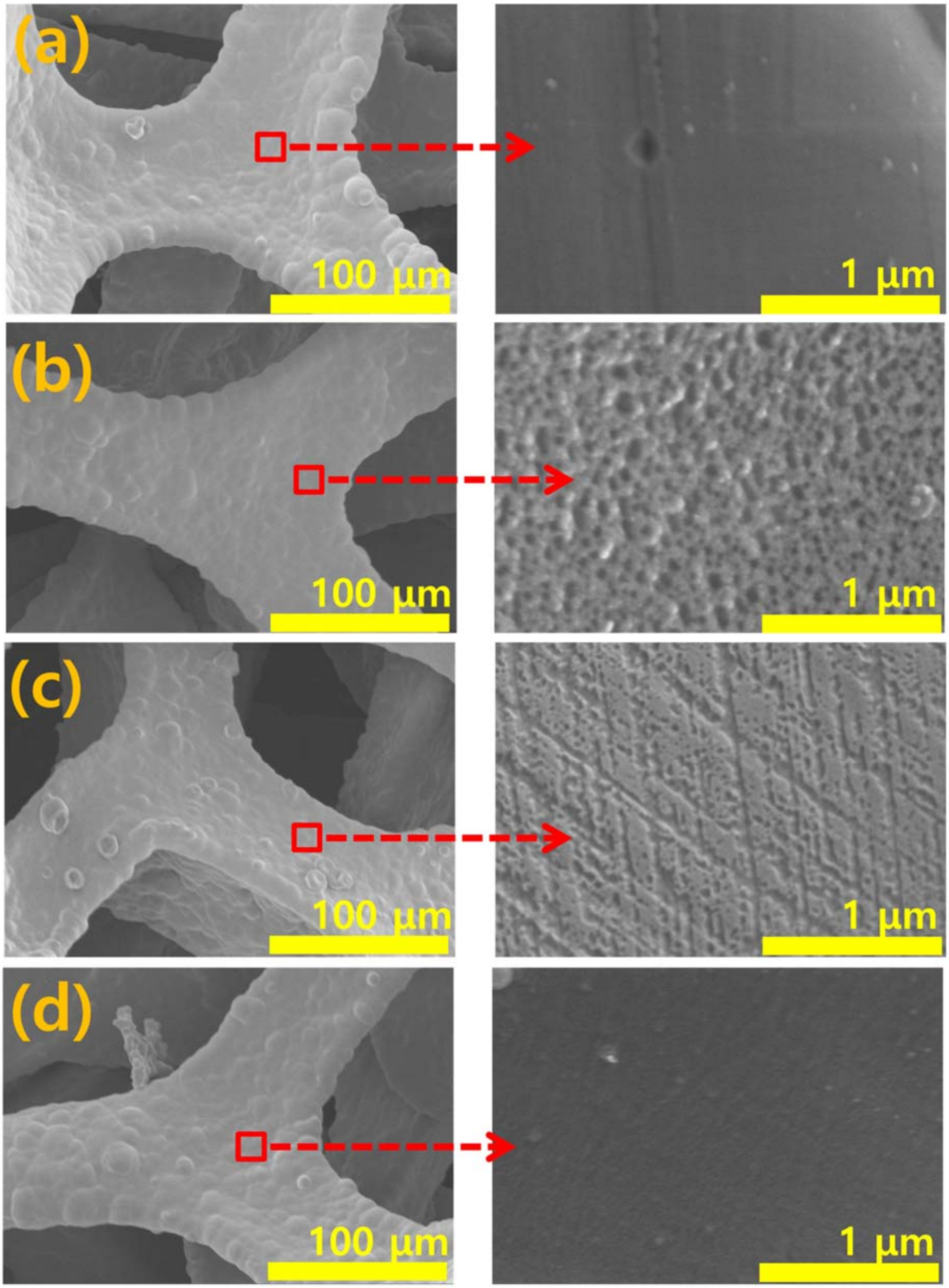

Fig. S6 SEM images of (a) NF-W, (b) NF-PS, (c) NF-H_2SO_4 and (d) NF-H_2O_2.

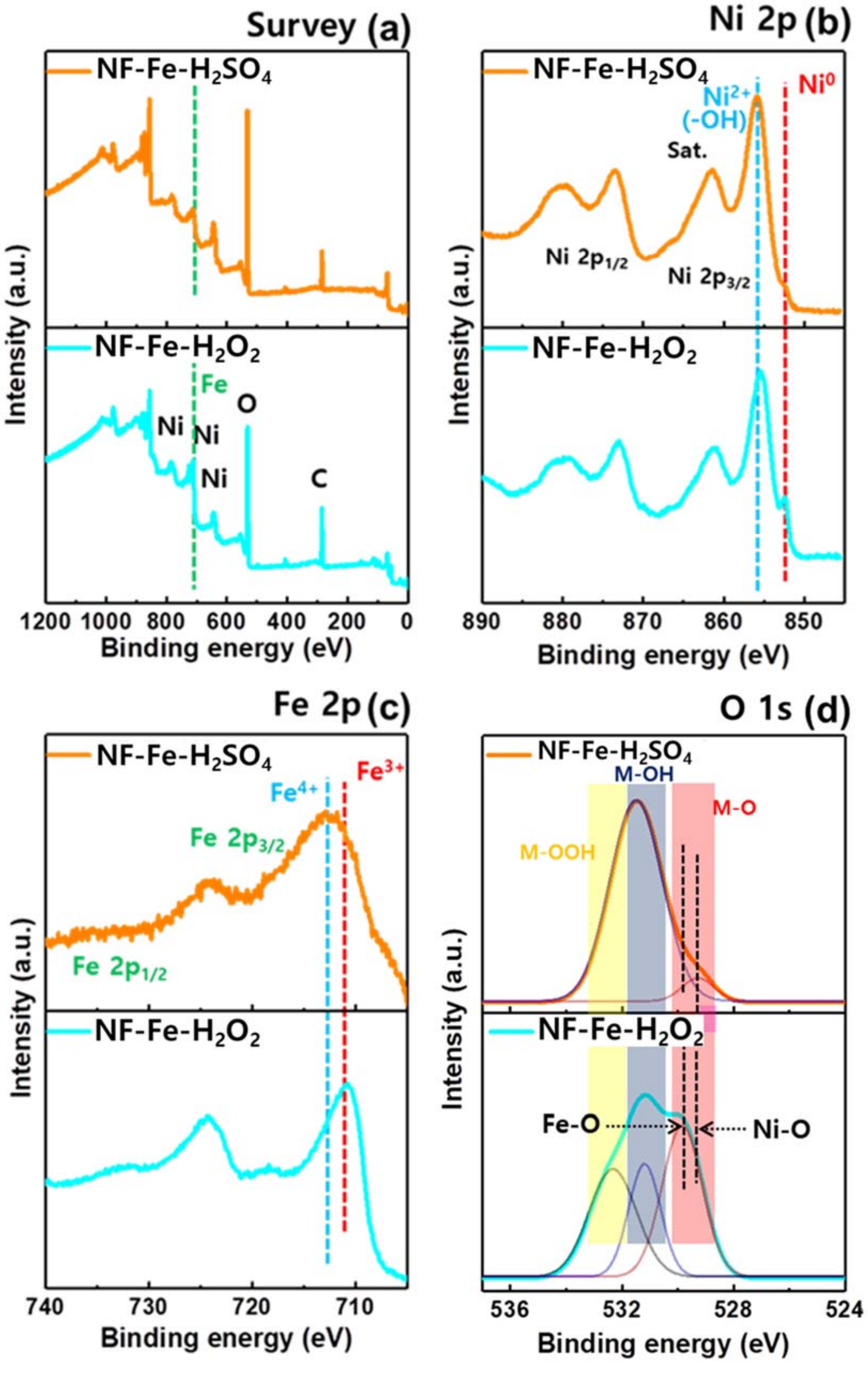

Fig. S7 (a) XPS survey scans and high resolution XPS spectra of (b) Ni 2p, (c) Fe 2p and (d) O 1s for different samples.

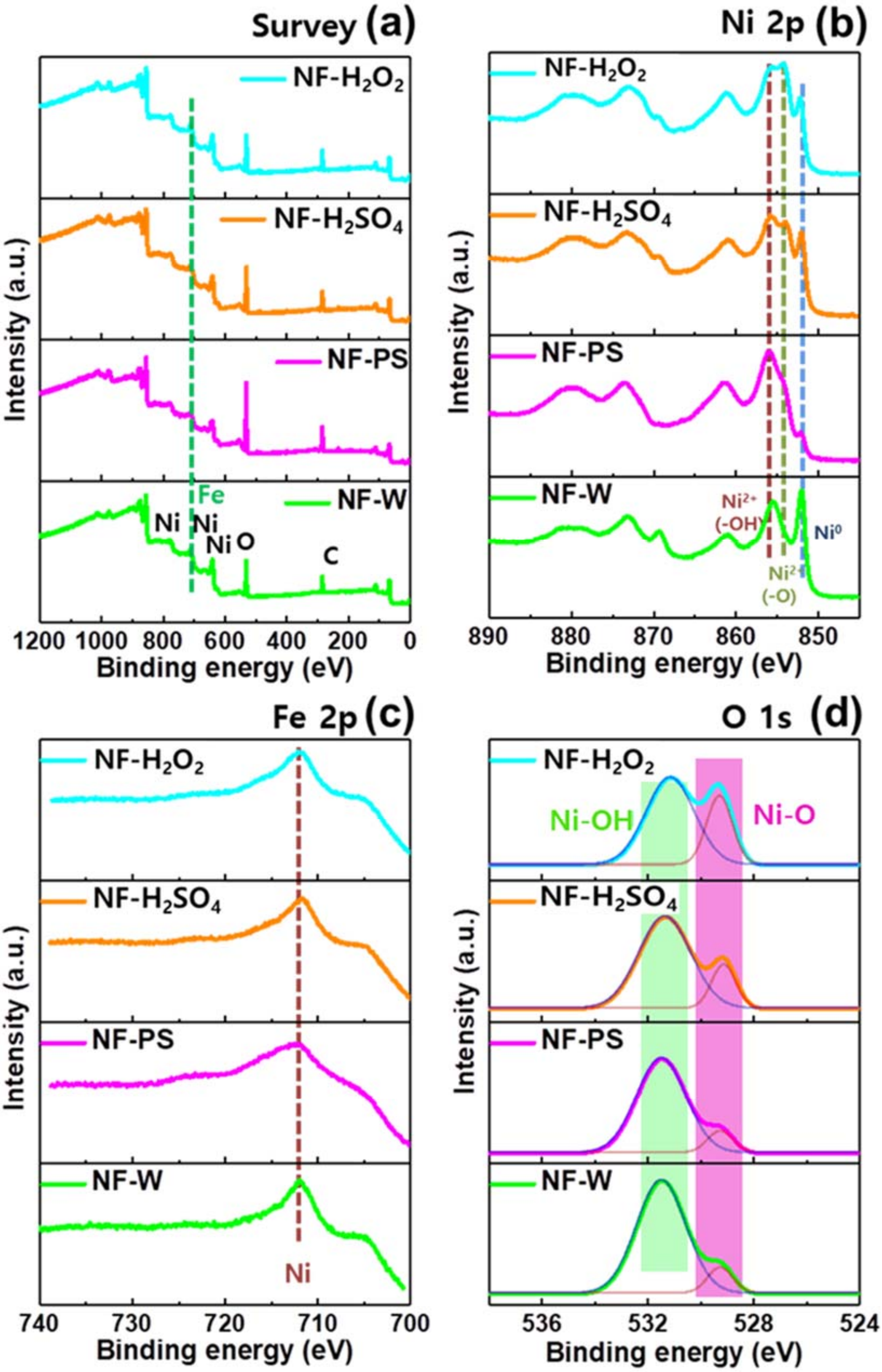

Fig. S8 (a) XPS survey scans and high resolution XPS spectra of (b) Ni 2p, (c) Fe 2p and (d) O 1s for different samples prepared without Fe precursor.

Table S1 Element compositions for different samples determined with XPS.

	O 1s (atom. %)	Ni 2p (atom.%)	Fe 2p (atom.%)
NF	53.88	46.12	0
NF-Fe-W	70.74	19.37	9.89
NF-Fe-PS	72.13	22.51	5.36
NF-Fe-H_2O_2	74.86	16.90	8.24
NF-Fe-H_2SO_4	67.24	29.80	2.96

Table S2 Element compositions for different samples prepared without Fe precursor determined with XPS.

	O 1s (atom. %)	Ni 2p (atom.%)
NF-W	52.63	47.37
NF-PS	67.90	32.10
NF-H_2O_2	54.20	45.80
NF- H_2SO_4	39.46	60.54

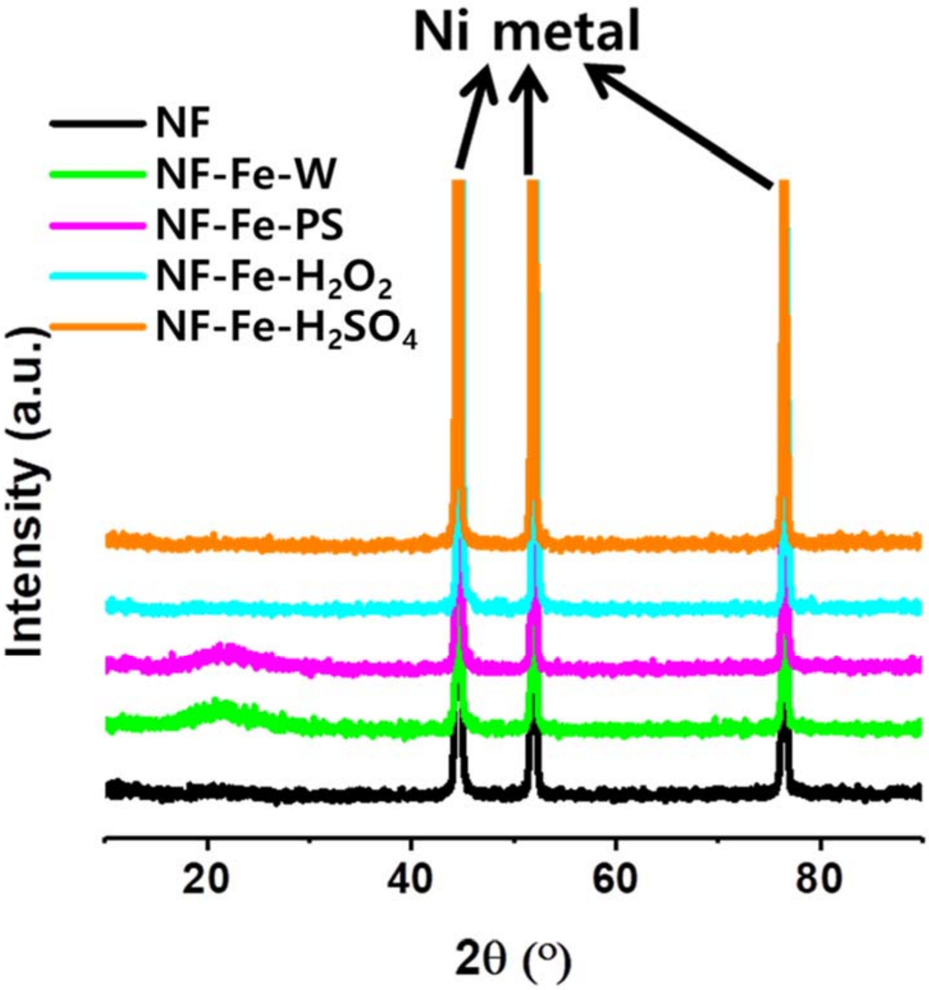

Fig. S9 XRD data of different NF-based samples.

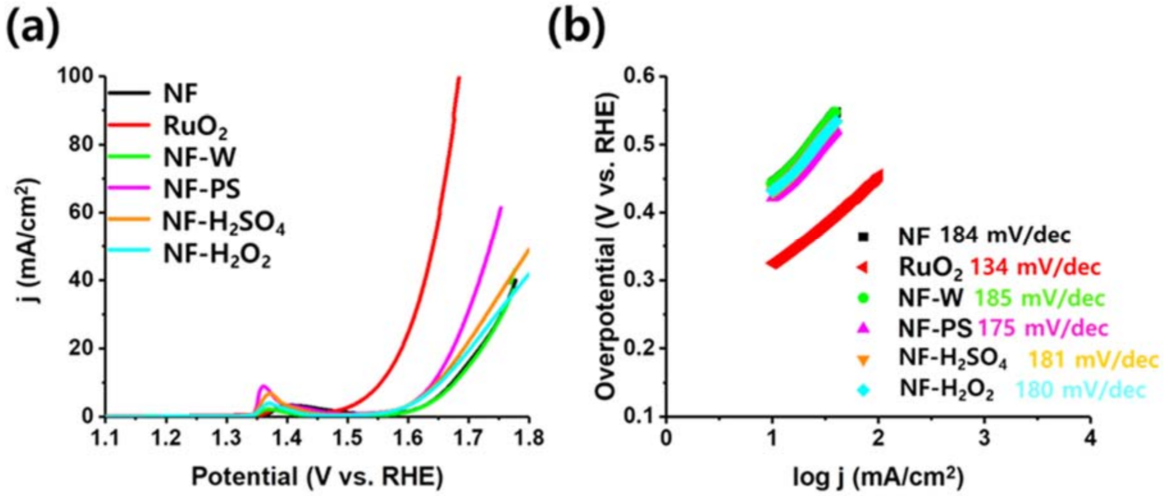

Fig. S10 (a) LSV curves of samples prepared in different media without Fe precursor and (b) Corresponding Tafel plots.

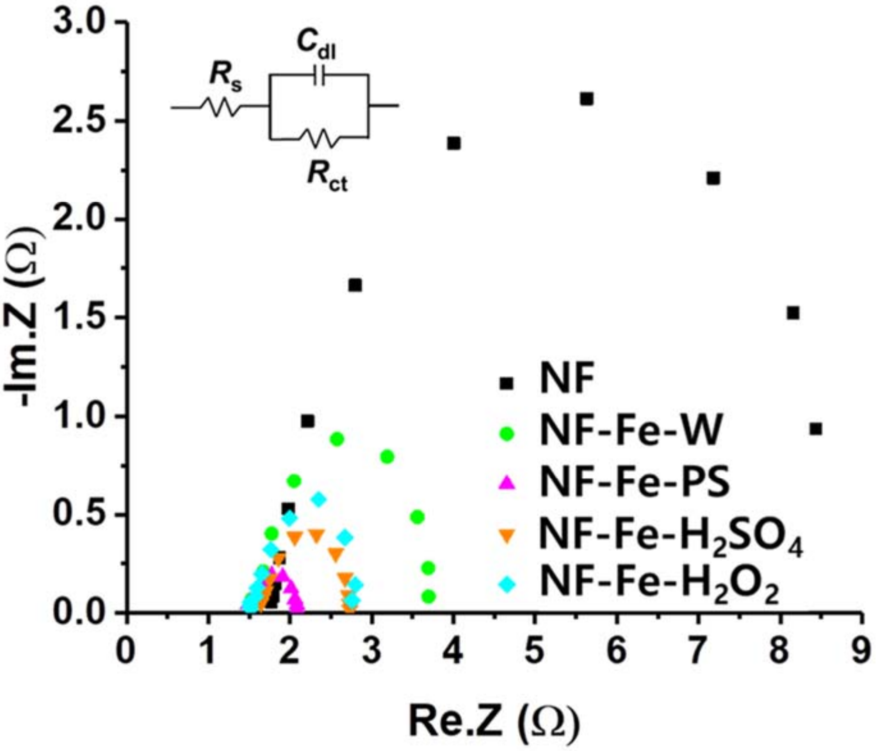

Fig. S11 Electrochemical Impedance spectra (EIS) of different samples. (Insert is a curcuit for EIS measurment.)

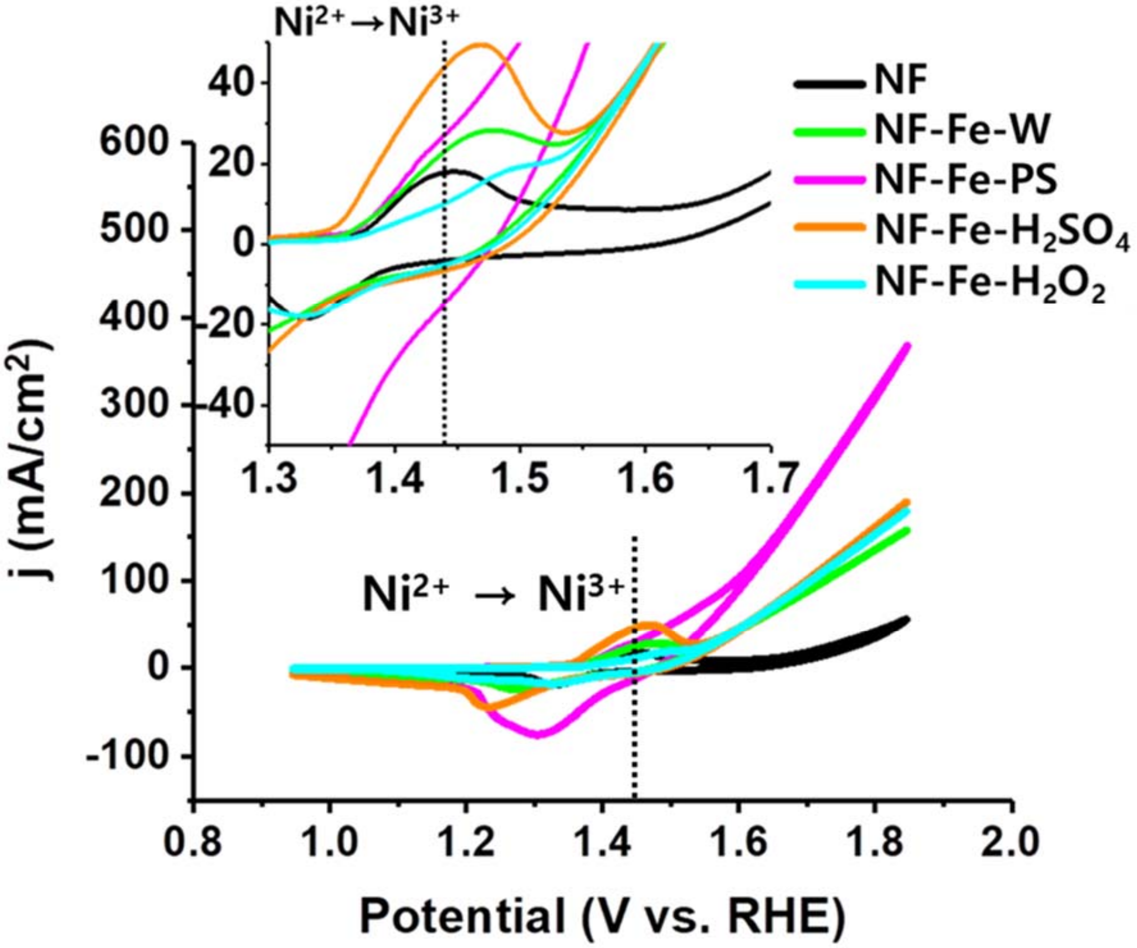

Fig. S12 CV curves of different samples measured in 1.0 M KOH electolyte. Scan rate is set to 20 mV/s for CV measurments.

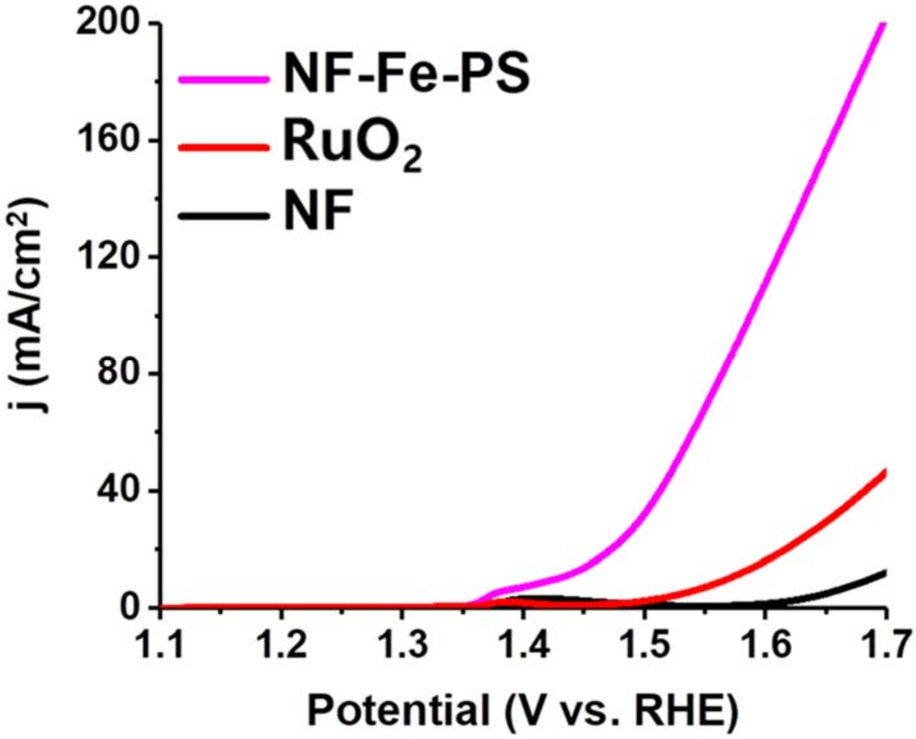

Fig. S13 LSV curves without iR correction.

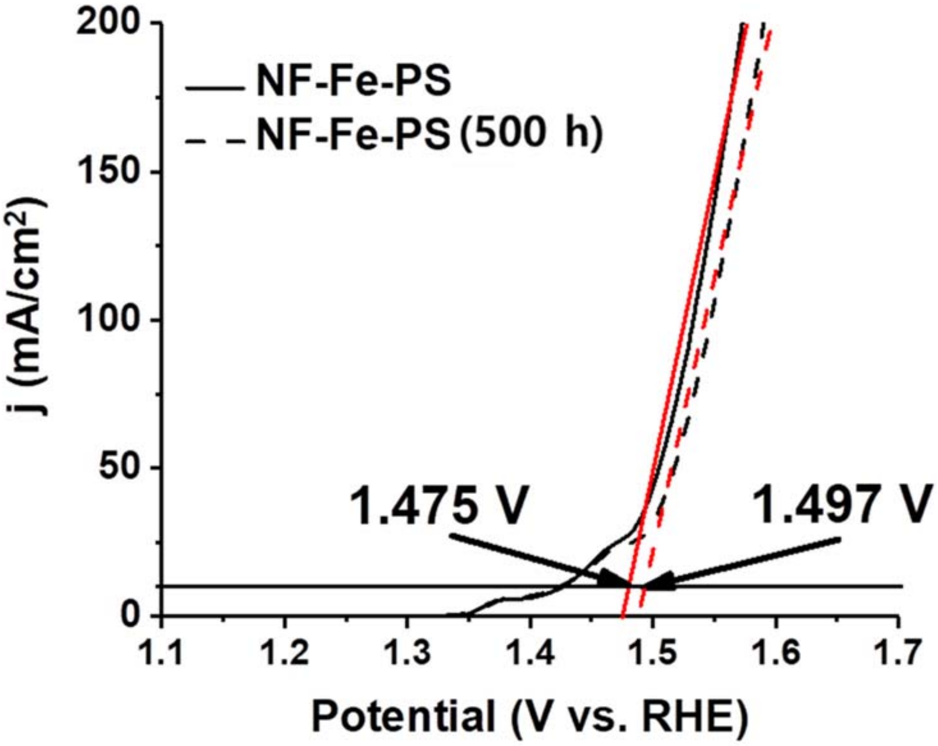

Fig. S14 LSV curves of NF-Fe-PS before and after long-term stability test.

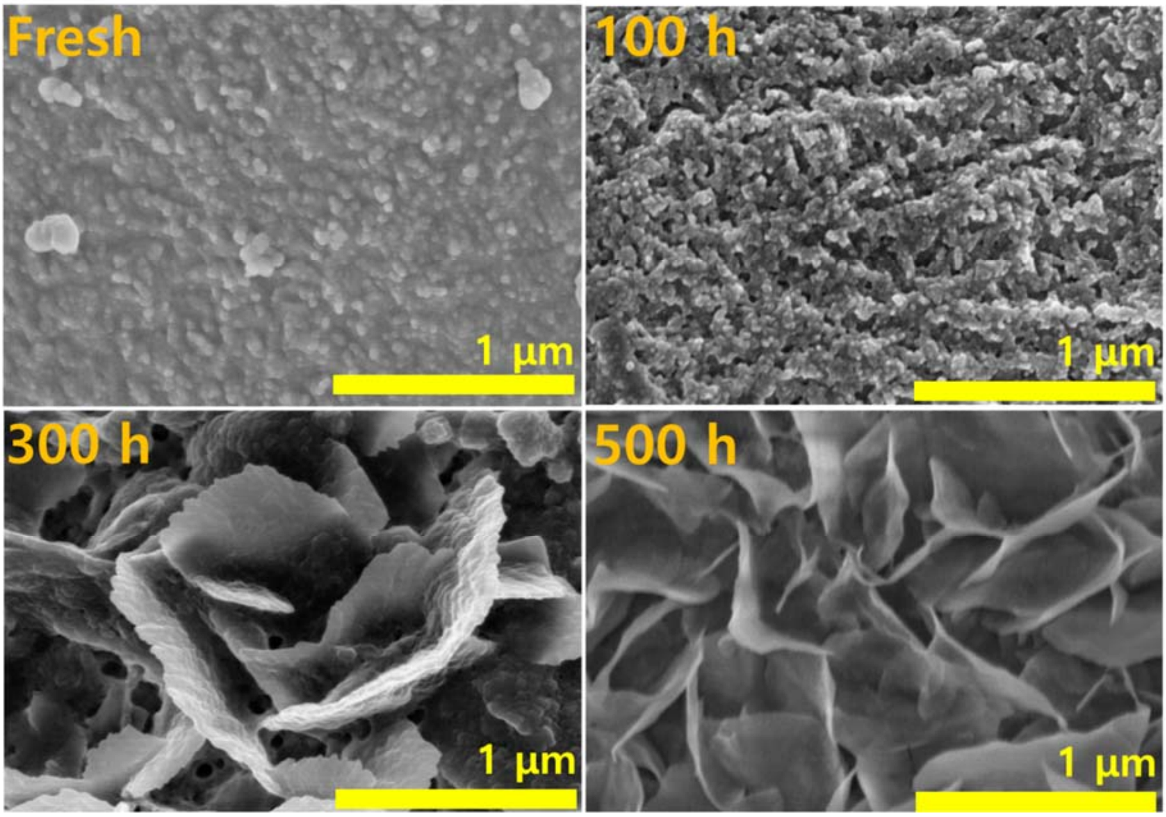

Fig. S15 SEM images of the NF-Fe-PS before and after long-term stability test for 100, 300 and 500 h, respectively.

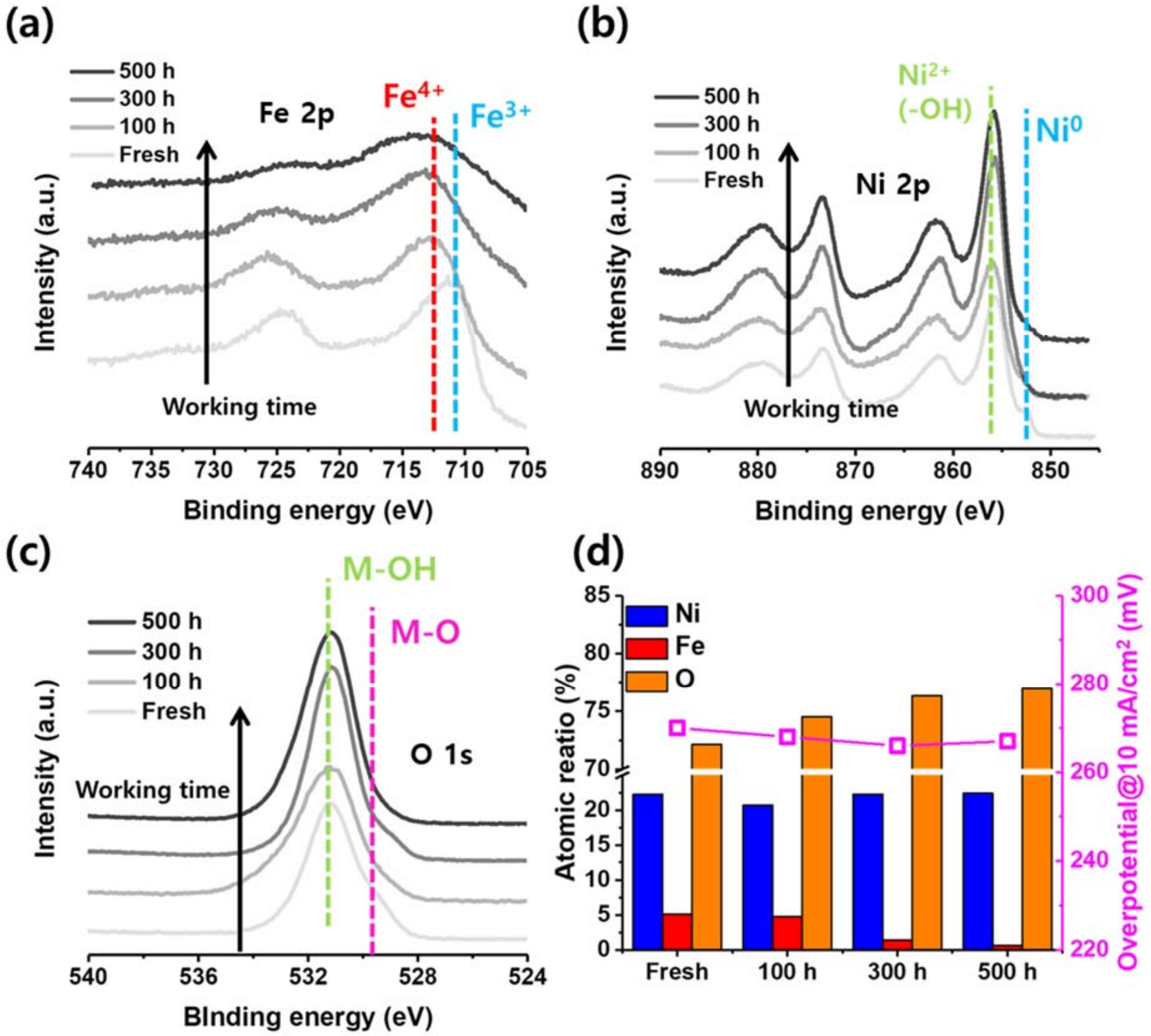

	O 1s (atom. %)	Ni 2p (atom.%)	Fe 2p (atom.%)	η@10mA/cm^2 (mV)
Fresh	72.13	22.27	5.16	270
100 h	74.50	20.70	4.80	268
300 h	76.31	22.30	1.39	266
500 h	76.94	22.40	0.66	267

Fig. S16 High resolution XPS spectra of (a) Fe 2p, (b) Ni 2p and (c) O 1s, and (d) elemental ratios determined from the XPS analysis along with OER activity of the as-prepared NF-Fe-PS before and after long-term stability test over different time periods. Bottom table summarize the corresponding element composition and overpotentials.

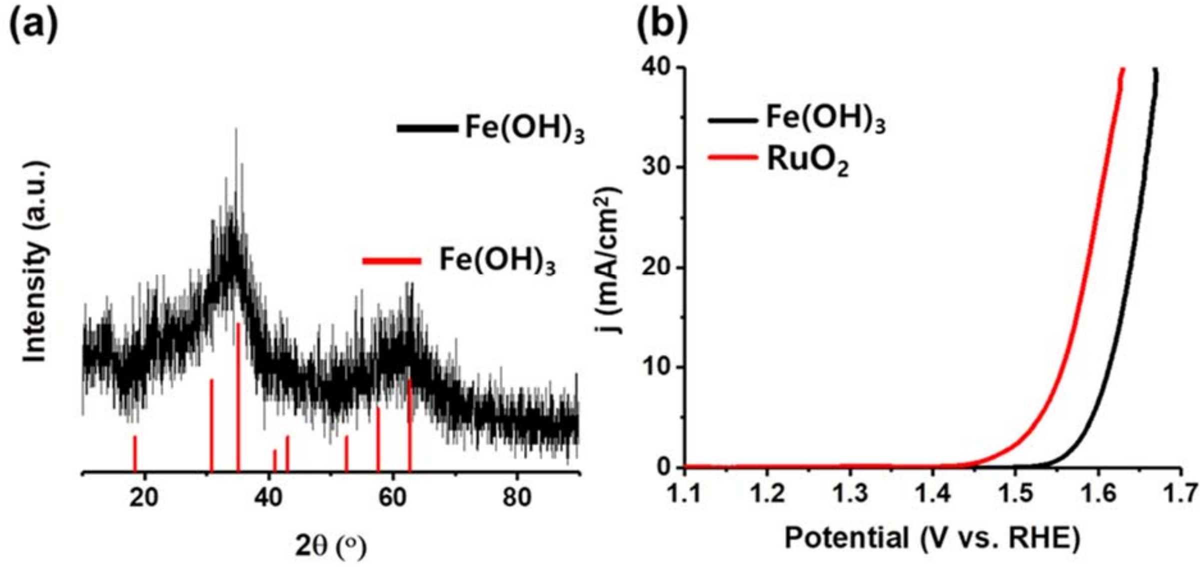

Fig. S17 (a) XRD patern and LSV curve of Fe(OH)$_3$.

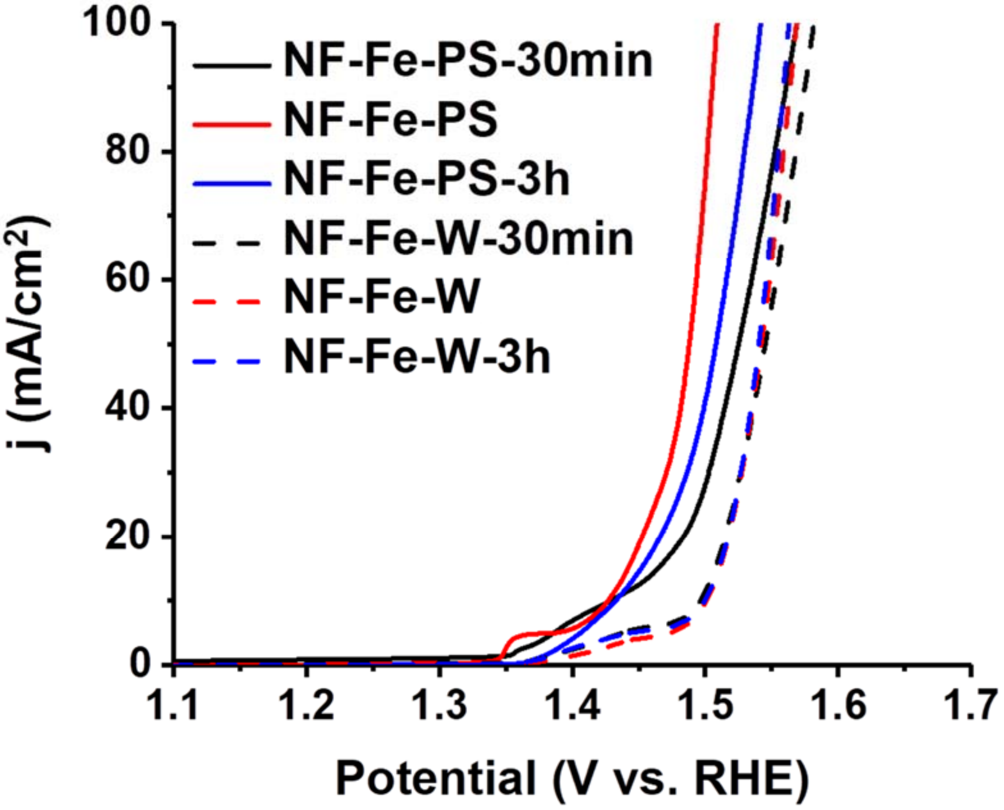

Fig. S18 OER LSV curves of samples prepared with different immersion time.

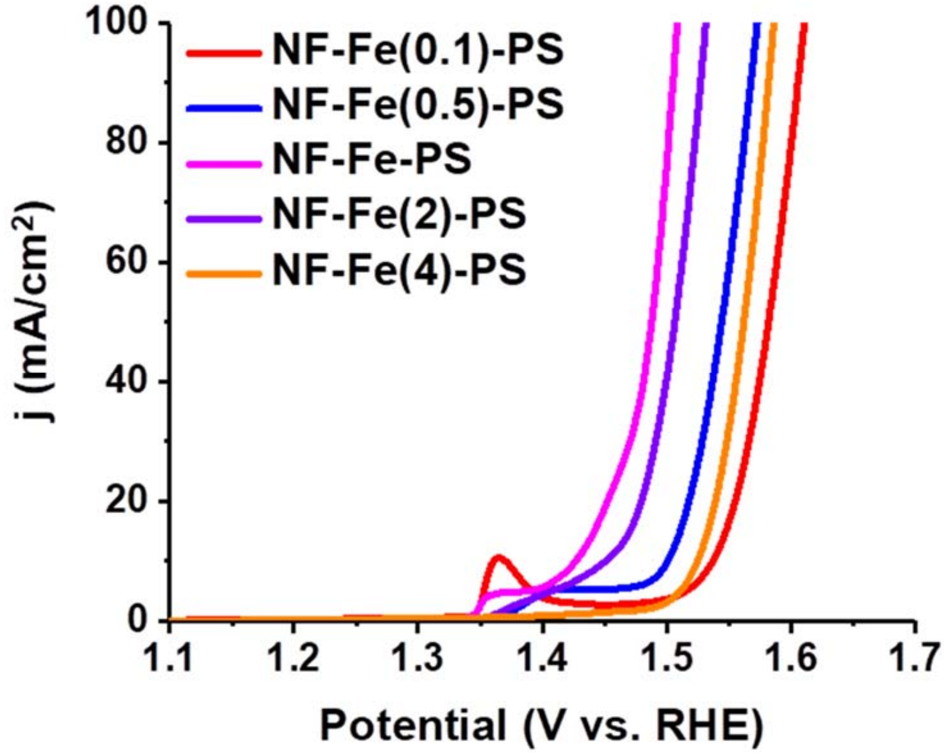

Fig. S19 OER LSV curves of samples prepared with different Fe amounts during synthesis.

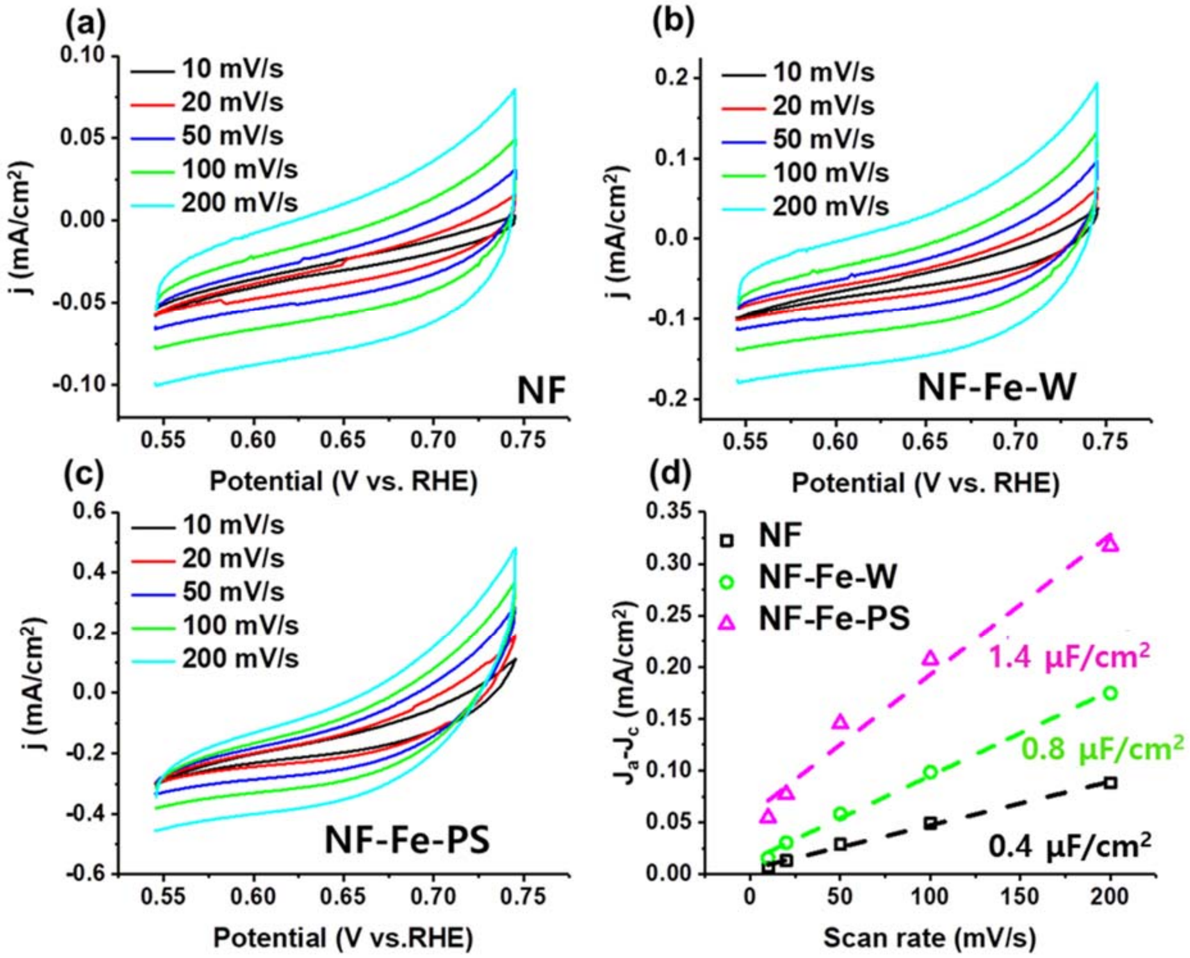

Fig. S20 (a)-(c) CV curves for different samples at various scan rates. (d) Calculated double layer capacitance from (a)-(c) at 0.65 V**.**

Reference

1. V. I. Anisimov, F. Aryasetiawan and A. I. Lichtenstein, J. Phys. Condens. Matter, 1997, 9, 767–808.

2. D. Friebel, M. W. Louie, M. Bajdich, K. E. Sanwald, Y. Cai, A. M. Wise, M.-J. Cheng, D. Sokaras, T.-C. Weng, R. Alonso-Mori, R. C. Davis, J. R. Bargar, J. K. Nørskov, A. Nilsson and A. T. Bell, J. Am. Chem. Soc., 2015, 137, 1305–1313.

3. S. Grimme, J. Antony, S. Ehrlich and H. Krieg, J. Chem. Phys., 2010, 132, 154104.